

# Mid-IR multiwavelength difference frequency generation based on fiber lasers

Jian Jiang<sup>1</sup>, Jianhua Chang<sup>1</sup>, Sujuan Feng<sup>1</sup>, Li Wei<sup>2</sup>, and Qinghe Mao<sup>1\*</sup>

<sup>1</sup>Anhui provincial Key Lab of Photonics Devices and Materials, Anhui Institute of Optics and Fine Mechanics, Chinese Academy of Sciences, Hefei, 230031, China

<sup>2</sup>Department of Physics & Computer Science, Wilfrid Laurier University, Waterloo, Ontario N2L 3C5, Canada  
\*mqinghe@atofm.ac.cn

**Abstract:** A mid-IR multiwavelength difference frequency generation (DFG) laser source with fiber laser fundamental lights is demonstrated by using the dispersion property of PPLN to broaden the quasi-phase-matching (QPM) acceptance bandwidth (BW). Our results show that the QPM BW for the pump YDFL is much larger than that for the signal EDFL. Using a multiwavelength YDFL and a single-wavelength EDFL as the pump and the signal lights, the DFG laser source can simultaneously emit 14 mid-IR wavelengths with the spacing of 14nm at a fixed PPLN temperature. Moreover, mid-IR multiwavelength lasing lines can be synchronously tuned between 3.28 and 3.47 $\mu$ m.

©2010 Optical Society of America

**OCIS codes:** (190.4360) Nonlinear optics, devices; (140.0140) Lasers and laser optics; (140.3510) Lasers, fiber

---

## References and links

1. D. Richter, A. Fried, B. P. Wert, J. G. Walega, and F. K. Tittel, "Development of a tunable mid-IR difference frequency laser source for highly sensitive airborne trace gas detection," *Appl. Phys. B* **75**(2-3), 281–288 (2002).
2. T. Tezuka, H. Ashizawa, M. Endo, S. Yamaguchi, K. Nanri, T. Fujioka, M. Takahashi, and S. Ohara, "Trace gas monitor based on difference frequency generation at 4 $\mu$ m using mass-production laser diodes as pump and signal light sources," *Appl. Phys. B* **78**(2), 229–233 (2004).
3. A. Straub, C. Gmachl, D. L. Sivco, A. M. Sergent, F. Capasso, and A. Y. Cho, "Simultaneously at two wavelengths (5.0 and 7.5 $\mu$ m) singlemode and tunable quantum cascade distributed feedback lasers," *Electron. Lett.* **38**(12), 565–567 (2002).
4. M. Asobe, O. Tadanaga, T. Umeki, T. Yanagawa, Y. Nishida, K. Magari, and H. Suzuki, "Unequally spaced multiple mid-infrared wavelength generation using an engineered quasi-phase-matching device," *Opt. Lett.* **32**(23), 3388–3390 (2007).
5. T. Umeki, M. Asobe, Y. Nishida, O. Tadanaga, K. Magari, T. Yanagawa, and H. Suzuki, "Widely tunable 3.4  $\mu$ m band difference frequency generation using apodized  $X^{(2)}$  grating," *Opt. Lett.* **32**(9), 1129–1131 (2007).
6. M. H. Chou, K. R. Parameswaran, M. M. Fejer, and I. Brener, "Multiple-channel wavelength conversion by use of engineered quasi-phase-matching structures in LiNbO<sub>3</sub> waveguides," *Opt. Lett.* **24**(16), 1157–1159 (1999).
7. Y. L. Lee, Y. C. Noh, C. Jung, T. J. Yu, B. A. Yu, J. Lee, D. K. Ko, and K. Oh, "Reshaping of a second-harmonic curve in periodically poled Ti: LiNbO<sub>3</sub> channel waveguide by a local-temperature-control technique," *Appl. Phys. Lett.* **86**(1), 011104 (2005).
8. M. H. Chou, I. Brener, K. R. Parameswaran, and M. M. Fejer, "Stability and Bandwidth Enhancement of Difference Frequency Generation (DFG)-based wavelength conversion by pump detuning," *Electron. Lett.* **35**(12), 978–980 (1999).
9. T. Yanagawa, H. Kanbara, O. Tadanaga, M. Asobe, H. Suzuki, and J. Yumoto, "Broadband difference frequency generation around phase-match singularity," *Appl. Phys. Lett.* **86**(16), 161106 (2005).
10. Z. Cao, L. Han, W. Liang, L. Deng, H. Wang, C. Xu, W. Chen, W. Zhang, Z. Gong, and X. Gao, "Broadband difference frequency generation around 4.2  $\mu$ m at overlapped phase-match conditions," *Opt. Commun.* **281**(14), 3878–3881 (2008).
11. D. Zheng, L. A. Gordon, Y. S. Wu, R. S. Feigelson, M. M. Fejer, R. L. Byer, and K. L. Vodopyanov, "16-microm infrared generation by difference-frequency mixing in diffusion-bonded-stacked GaAs," *Opt. Lett.* **23**(13), 1010–1012 (1998).
12. D. E. Zelmon, D. L. Small, and D. Jundt, "Infrared corrected Sellmeier coefficients for congruently grown lithium niobate and 5 mol. magnesium oxide doped lithium niobate," *J. Opt. Soc. Am. B* **14**(12), 3319–3322 (1997).
13. Q. H. Mao, Z. J. Zhu, Q. Sun, W. Q. Liu, and J. W. Y. Lit, "Influences of gain broadening on multiwavelength oscillations in YDFLs and EDFLs," *Opt. Commun.* **281**(11), 3153–3158 (2008).

14. Q. H. Mao, J. Jiang, X. Q. Li, J. H. Chang, and W. Q. Liu, "Widely tunable continuous wave mid-IR DFG source based on fiber lasers and amplifiers," *Laser Phys. Lett.* **6**(9), 647–652 (2009).
15. Q. Mao, J. Wang, X. Sun, and M. Zhang, "A theoretical analysis of amplification characteristics of bi-directional erbium-doped fiber amplifiers with single erbium-doped fiber," *Opt. Commun.* **159**(1-3), 149–157 (1999).

## 1. Introduction

Continuous-wave 3-5 $\mu\text{m}$  mid-infrared (mid-IR) laser sources are very useful for applications in spectroscopy, optical sensing and detection [1,2]. To meet the requirements of multiple species synchronous or multi-lines detections, mid-IR multiwavelength laser sources are most important. In 2002, Straub et al. obtained dual-wavelength mid-infrared lasing lines near 5.0 and 7.5  $\mu\text{m}$  using a quantum cascade laser with the distributed feedback structure specially designed [3]. However, such a dual-wavelength quantum cascade laser may have to operate at very low temperature, and the wavelength spacing is also too large to achieve more lasing lines. In order to obtain more lasing lines in the mid-IR region, in 2007, Asobe et al. demonstrated a mid-IR three-wavelength difference frequency generation (DFG) laser source based on the quasi-phase matching (QPM) technique, which uses a periodically poled LiNbO<sub>3</sub> (PPLN) waveguide as the nonlinear crystal and a DFB laser diode array as the fundamental lights. The three lasing lines were then utilized in a multi-components synchronous detection system [4]. This indicates that the DFG technique may provide a promising method to achieve multiwavelength mid-IR radiations. However, when a DFG laser source operates in a multiwavelength mode, the QPM acceptance bandwidth (BW) of the nonlinear crystal should be large enough to ensure the multiple fundamental lights satisfy the QPM condition simultaneously. Unfortunately, the BW of normal uniform grating PPLNs is only about 1-10 $\text{cm}^{-1}$ . Thus, when PPLNs is used as the nonlinear crystal for a mid-IR multiwavelength DFG laser source, the BW has to be broadened. To date, several approaches, such as chirped [5], phase modulation [6], temperature-gradient control [7], and detuning the pump from the degenerate phase match wavelength [8], have been proposed to increase the QPM BW of PPLNs. In particular, by using the dispersion property [9,10], the QPM BW of PPLN has successfully been increased to be more than 100  $\text{cm}^{-1}$  near 2 or 4 $\mu\text{m}$  for mid-IR single-wavelength widely tuning operation. However, there is no mid-IR multi-wavelength radiation source with widely tuning function near 3 $\mu\text{m}$  available, where many gas molecules exhibit fundamental rotation and vibration absorptions in this mid-IR region.

In this paper, we demonstrate a tunable multiwavelength mid-IR DFG laser source with fiber laser fundamental lights for the first time to our best knowledge. The fiber lasers are ytterbium- and erbium-doped fiber lasers, which can both emit multiple lasing lines near 1060 and 1550nm, respectively. We shall show how to broaden the QPM BW of a normal uniform grating PPLN for such a DFG laser source by using the dispersion property of PPLN, and which one should operate in multiwavelength mode for the two fiber laser fundamental lights. With a multiwavelength ytterbium-doped fiber laser (YDFL) as the pump light and a single wavelength erbium-doped fiber laser (EDFL) cascaded by an erbium-doped fiber amplifier (EDFA) as the signal light, our DFG laser source, which is based on a uniform grating PPLN can simultaneously emit 14 lasing lines with the spacing about 14nm near 3.3 $\mu\text{m}$  when the temperature of the PPLN is fixed at 73.5 $^{\circ}\text{C}$ . Moreover, the multiwavelength mid-IR lasing lines can be tuned synchronously between 3.28 and 3.47 $\mu\text{m}$  by changing the wavelength of the signal light.

## 2. QPM acceptance bandwidth

For Gaussian fundamental light beams, the idler power exited from a DFG laser source based on the QPM technique is proportional to  $\sin^2(\Delta k L/2)$  [11], where  $\Delta k$  represents the wave vector mismatch, and  $L$  is the length of nonlinear crystal. If  $\Delta k_{FWHM}$  is defined as the full width at half maximum (FWHM) of the wave vector mismatch, then, we have  $\Delta k_{FWHM} = 0.8858\pi/L$ .

On the other hand, the wave vector mismatch may be written as

$$\Delta k = 2\pi \left( n_p / \lambda_p - n_s / \lambda_s - n_i / \lambda_i - 1 / \Lambda \right) \quad (1)$$

where  $\Lambda$  is the grating period of the crystal;  $\lambda_{p,s,i}$  and  $n_{p,s,i}$  are the wavelengths and the refractive indices of the pump, signal and idler, respectively.  $n_{p,s,i}$  is usually functions of the wavelength and crystal temperature, and can be obtained numerically from published Sellmeier fits for PPLN [12].

When  $|\Delta k| \leq |\Delta k_{FWHM}|$ , the QPM condition is satisfied. Thus, the FWHM bandwidth in  $\lambda_{p,s,i}$  may be found by

$$\left| 2\pi \left( n_p / \lambda_p - n_s / \lambda_s - n_i / \lambda_i - 1 / \Lambda \right) \right| = 0.8858\pi / L \quad (2)$$

With Eq. (2), the QPM properties of the DFG laser source with the YDFL and EDFL as pump and signal lights may be simulated.

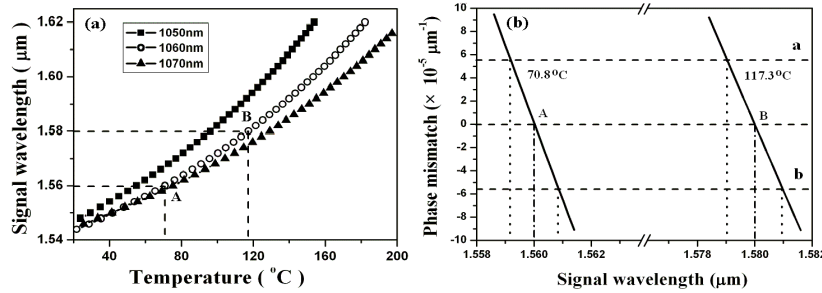


Fig. 1. (a) Signal wavelength as a function of crystal temperature under perfect QPM condition for different given pump wavelengths; (b) Phase mismatch as a function of the signal wavelength with the pump wavelength of 1060nm for different given crystal temperatures.

Figure 1(a) shows the simulation result of  $\lambda_s$  satisfying the perfect phase matching as a function of the crystal temperature for different fixed  $\lambda_p$ . We use the PPLN length of 50mm throughout our simulations. As seen from the figure, for a given  $\lambda_p$ , the signal wavelength ( $\lambda_s$ ), which can satisfy the perfect phase matching, is uniquely determined by the crystal temperature. The signal wavelength under the perfect phase matching increases monotonously with the crystal temperature. When the pump wavelength is 1060nm, the signal wavelengths under the perfect phase matching at 70.8 and 117.3°C are 1560 and 1580nm, corresponding to Points A and B in Fig. 1(a). However, for a fixed pump wavelength, when the crystal temperature is set at a value to make a specific signal wavelength to satisfy the perfect phase matching, the wave vector mismatch caused by the signal wavelength variation near the perfect phase matching signal wavelength may still be less than  $\Delta k_{FWHM}$ , so the QPM condition can be still satisfied. Figure 1(b) shows the wave vector mismatch as a function of the signal wavelength for the pump wavelength of 1060nm with the crystal temperatures being set at 70.8 and 117.3°C, respectively. As seen in the figure, the wave vector mismatches for the signal wavelengths of 1560 and 1580nm are zero. When the signal wavelengths vary between 1559.2 and 1560.2nm and 1579-1580.9nm, the wave vector mismatches are still less than  $\Delta k_{FWHM}$ , i.e., within Dash lines a and b, the QPM condition can still be satisfied. However, the QPM BW for the signal, which is defined as the signal wavelength variation range allowed by the QPM condition, is less than 2nm. Similar simulations for other pump wavelengths in the YDF gain band also show that the QPM BW for the signal is very narrow, typically about 2nm.

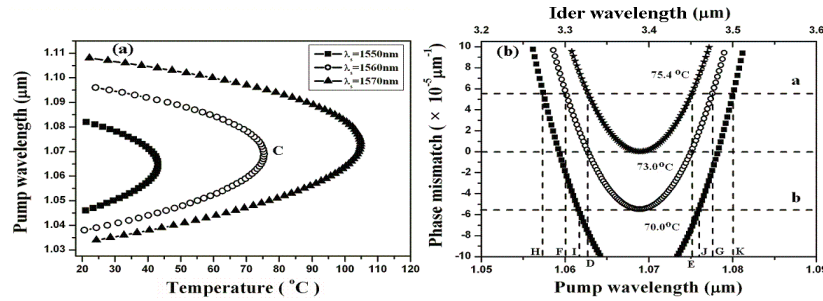


Fig. 2. (a) Pump wavelength as a function of the crystal temperature under perfect QPM condition for different given signal wavelengths; (b) Phase mismatch as a function of the pump wavelength with the signal wavelength of 1560nm for different given crystal temperatures.

Figure 2(a) shows the perfect phase matched pump wavelength as a function of the crystal temperature when the signal wavelength is fixed. For any given signal wavelength, as shown in the figure, the perfect phase-matched pump wavelength no longer increases monotonously with the crystal temperature. Instead, for a given crystal temperature, there are two perfect phase-matched pump wavelengths. As the crystal temperature increases, the two perfect phase-matched pump wavelengths are gradually close to each other and finally overlapped where the crystal temperature reaches its maximum for the specific signal wavelength. For the given signal wavelength of 1560nm, for example, the maximum crystal temperature is 75.4°C, where the overlapped perfect phase-matched pump wavelength is 1069nm [Point C in Fig. 2(a)].

Figure 2(b) shows the QPM BW at different crystal temperatures for the pump near 1069nm and the signal wavelength at 1560nm. It can be clearly seen that, when the crystal temperature is set at 75.4°C, the wave vector mismatch for the pump wavelength of 1069nm is zero, however, the BW for the pump, given by the condition that the wave vector mismatch is less than  $\Delta k_{FWHM}$ , i.e., within lines a and b, is about 12nm, from 1063 to 1075nm (the range between Points D and E). When the crystal temperature is decreased to 73°C, the BW for the pump wavelength increases to 17nm, from 1061 to 1078nm (Points F and G). Since the relationship curve between the wave vector mismatch and the pump wavelength at 73°C is right tangent to Dash line b, the BW for the pump wavelength reaches its maximum. When the crystal temperature is further decreased to 70°C, the range of the QPM BW for the pump wavelength is split into two individual regions, which are between Points H and I, and J and K, respectively, shown in the figure. However, both the individual regions are narrow, only about 4nm. Our simulation results for other signal wavelengths in the gain bandwidth of EDF also show that the QPM BW for the pump wavelength exhibits the similar properties described above. By making use of its dispersion properties to optimize the crystal temperature, the QPM BW for the pump wavelength may be broadened as large as 10-20nm.

According to our simulation results, thus, when EDFL and YDFL located in 1550 and 1060nm regions are respectively used as the fundamental lights for a multiwavelength or tunable DFG laser source, the YDFL should be chosen to operate in multiwavelength mode because the QPM BW for the pump light is much larger than that for the signal.

### 3. Experimental setup

Figure 3(a) shows the schematic configuration of our mid-IR multiwavelength DFG laser source, which consists of three parts: a pump source, a signal source and DFG unit. The pump source is a multiwavelength YDFL, and its configuration is shown in Fig. 3(b) [13]. An optical isolator (ISO) is inserted into the ring cavity of the YDFL to ensure the unidirectional propagation in the cavity. A 975nm laser diode (LD) with the maximum power of 200mW is used as the pump, which is launched into the YDF through a wavelength division multiplexing (WDM) coupler. The YDF has the absorption of 199dB/m at 975nm and length of 5m. A Sagnac loop based on 3dB optical coupler (OC1), with a piece of PMF and a

polarization controller (PC4) being inserted into the loop, is used as the comb filter to generate the multiwavelength oscillation. Another PC with the label of 3 is used to control the polarization state of the input light of the Sagnac loop. A 90:10 optical coupler (OC2) is used for the laser output. Figure 3(c) shows the measured output spectrum of the multiwavelength YDFL, which simultaneously emits 15 lasing lines with the spacing of about 1.4nm between 1055.3 and 1074.8nm, and the individual linewidth of about 0.1nm. The total output power of YDFL is about 15mW. An EDFL with linear cavity cascaded with an EDFA is used as the signal light [14]. The EDFL has the central wavelength near 1560nm and the output power of 12mW. The EDFA is bidirectional pumped with a 980nm LD and a 1480nm LD for obtaining both low noise and high output power [15]. The total power of the signal source after having been amplified by the EDFA is about 150mW. With two polarization controllers (PC1 and PC2) to adjust the polarization states, the pump and the signal beams are combined with a 1060/1550 WDM fiber coupler, then collimated with a grin-lens at the fiber facet, and finally launched into the DFG unit with a 100mm focal length plano-convex lens (M1). The nonlinear crystal is a PPLN with the grating period of 30 $\mu$ m, which are 50, 1 and 1mm in length, width and thickness, respectively. The crystal is posited in a temperature controller, which can be adjusted in the range between 0 $^{\circ}$ C and 200  $^{\circ}$ C with a precision of  $\pm$  0.1  $^{\circ}$ C. The residual pump and signal lights are blocked with a Ge filter, and the generated mid-IR radiation is delivered with a 100mm CaF<sub>2</sub> lens (M2) to a Fourier transform Infrared spectroscopy (FTIR) for measurements.

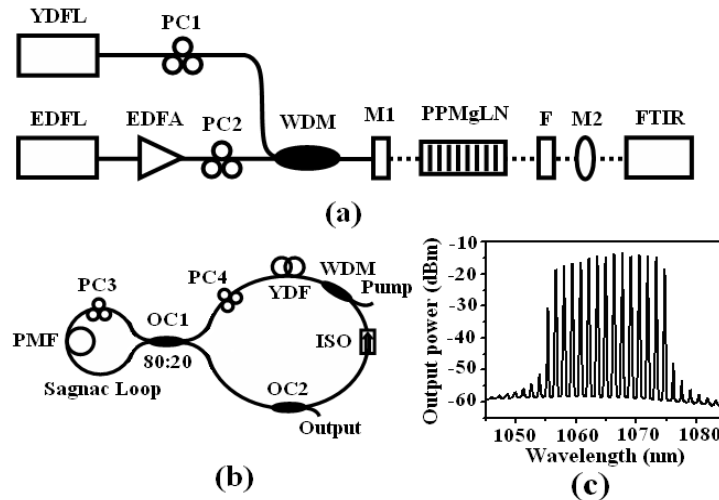


Fig. 3. (a) Schematic diagram of the mid-IR multiwavelength DFG laser source; (b) Configuration of the multiwavelength YDFL; (c) Measured multiwavelength output spectrum of the multiwavelength YDFL.

#### 4. Results and discussions

In our experiment the crystal temperature is first set at 73.5 $^{\circ}$ C. By suitably adjusting the PCs to optimize the polarization orientation of pump and signal lights, mid-IR multiwavelength radiation lines are simultaneously obtained with our DFG laser source. Figure 4(a) shows the measured output spectrum. As seen from the figure, 14 lasing lines with the wavelength spacing of 14nm are located in 2890-3055  $\text{cm}^{-1}$ , i.e., 3460-3273 nm, over a range of about 180nm. These 14 mid-IR lasing lines respectively correspond to the central 14 wavelengths of the multiwavelength YDFL pump lights shown in Fig. 3(c), indicating that mid-IR multiwavelength radiations may be obtained with the DFG method with a single wavelength EDFL near 1550nm as the signal light and a multiwavelength YDFL near 1060nm as the pump light because the QPM BW of the pump may be large enough to allow the

multiwavelength pump lights satisfy the QPM condition simultaneously for a fixed crystal temperature.

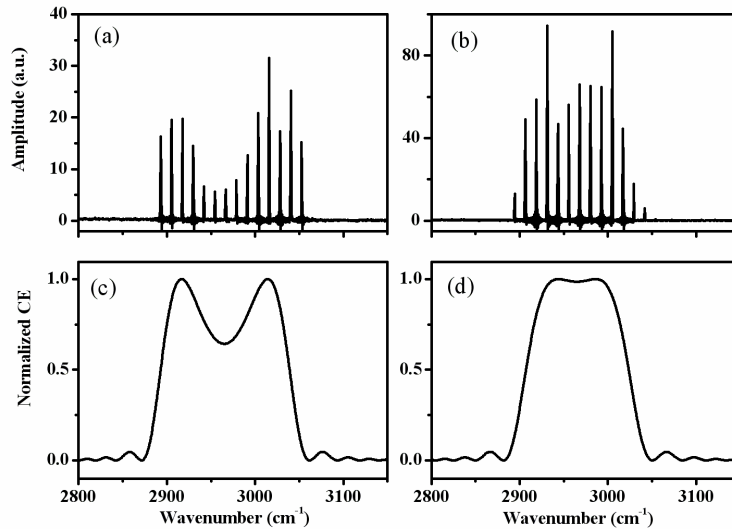


Fig. 4. Measured output spectrum of the DFG laser source with (a)  $T = 73.5^{\circ}\text{C}$  and (b)  $T = 75^{\circ}\text{C}$ , and calculated normalized conversion efficiency with (c)  $T = 73.5^{\circ}\text{C}$  and (d)  $T = 75^{\circ}\text{C}$ .

However, the measured mid-IR multiwavelength lasing lines shown in Fig. 4(a) are not flat, and the amplitudes of the central several lasing lines are relative low though the amplitudes of the corresponding pump lines are high [see Fig. 3(c), in dB scale]. This indicates that the conversion efficiencies for the pump lasing lines are different though they are all in the QPM BW. In fact, the crystal temperature affects not only the QPM BW for the pump but also the phase mismatch of each pump wavelength in it, which in turn affects the conversion efficiency. Figure 4(b) shows the measured output spectrum of our DFG laser source when the crystal temperature is set at  $75^{\circ}\text{C}$  and the other conditions are the same as Fig. 4(a). This time the number of the mid-IR lasing lines is 13. The amplitudes of these 13 lasing lines are relatively flat compared to that shown in Fig. 4(a). Note that one line is missed here probably because the QPM BW for the pump at  $75^{\circ}\text{C}$  is decreased; this can be seen from Figs. 4(c), 4(d) in which calculated normalized conversion efficiencies (CE) with the same crystal temperatures as those in Figs. 4(a), 4(b) are given. Figure 4 also indicates that the experimental results are in agreement with the simulation results.

On the other hand, owing to the broadband QPM BW, our Mid-IR laser source can still maintain multiwavelength output within a certain range by changing the signal wavelength, accompanied with suitable adjustment of the crystal temperature and the polarization controller of PC2. Figure 5(a) shows the measured output spectrum of the DFG laser source when the signal wavelength and the crystal temperature are changed to 1548nm and  $34.2^{\circ}\text{C}$ , respectively, keeping the other conditions the same as those in Fig. 4(b). As seen in Fig. 5(a), although the number of the mid-IR lasing lines is decreased to 11, they have moved to long wavelength band, located in  $2876\text{-}3000\text{ cm}^{-1}$ , i.e.,  $3476\text{-}3334\text{ nm}$ . Similarly, when the signal wavelength and the crystal temperature are moved to 1580nm and  $129.3^{\circ}\text{C}$ , there are still 8 lasing lines existing in the output spectrum, as illustrated in Fig. 5(b). This indicates that, when the signal wavelength is changed in a certain range, the QPM BW for the pump is still large enough to emit simultaneously multiwavelength mid-IR radiations. Our experiment results show that at least 8 tunable multiwavelength mid-IR lasing lines between  $3.28$  and  $3.47\mu\text{m}$  can be achieved synchronously when the signal wavelength is varied between 1548 and 1580 nm with the optimized crystal temperature and PC2 to adapt the change of the signal wavelength.

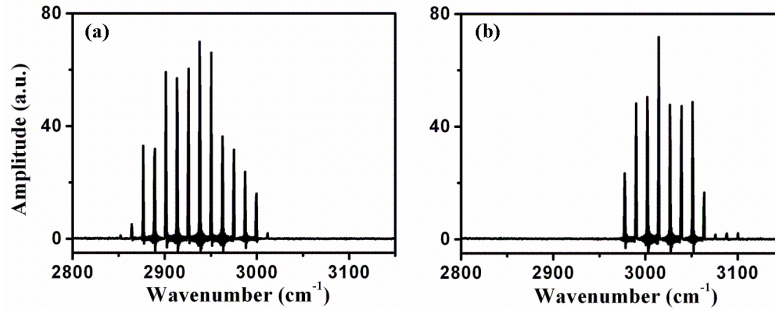


Fig. 5. Measured output spectrum of the DFG laser source, (a)  $\lambda_s = 1548\text{nm}$ ,  $T = 33.8^\circ\text{C}$ ; (b)  $\lambda_s = 1580\text{nm}$ ,  $T = 129.3^\circ\text{C}$ .

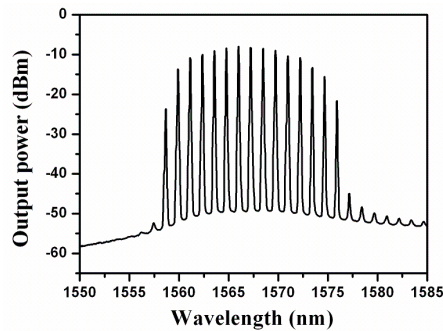


Fig. 6. Measured output spectrum of the multiwavelength EDFL cascaded by an EDFA.

Finally, the output properties of the DFG laser source are also experimentally investigated when a multiwavelength EDFL and a single wavelength YDFL, which have the same configurations described in section 3, are used as the fundamental lights. The central wavelength of the YDFL is 1064.9nm. The multiwavelength signal light consists of 15 lasing lines with the wavelength spacing of about 1.2nm in the region from 1558 to 1574nm, as seen from Fig. 6 which shows the output spectrum of the multiwavelength signal light after being amplified by the EDFA. With those signal and pump lights, the measured output spectrum of the DFG laser source is shown in Fig. 7 when the crystal temperature is set at 89.7°C. As seen in Fig. 7, only two mid-IR radiation lines with the wave number of 3000.1 and 3004.9  $\text{cm}^{-1}$ , corresponding to the wavelength of 3333.3 and 3327.9nm, are obtained simultaneously, though the incident signal light has 15 lasing lines. In our experiment, PC2 is adjusted to vary the polarization states of incident signal lines. No new mid-IR idler lines are generated. Only amplitude variations for the same two mid-IR lines are observed, indicating that the other incident signal lines may not locate in the QPM BW, because the incident multiwavelength signal lines are almost flattened. When the crystal temperature is changed, there is no new generated mid-IR idler lines except the variation of the wave-numbers of the two output mid-IR lines. This means that the special region of the signal light satisfying the QPM condition may change with the crystal temperature while the QPM BW for the signal is unchanged. Only about 2nm inferred from our experiment, which results in that the two signal lines participated in the DFG process successively switch among the incident signal lines. This experimental result is in agreement with the calculated normalized CE curves for different crystal temperature also given in Fig. 7.

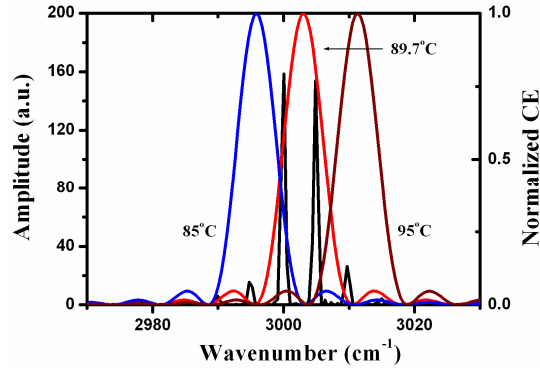


Fig. 7. Measured output spectrum of the DFG laser source and calculated normalized conversion efficiency (CE) curves for different crystal temperature.

Our experiments have shown that, when the fundamental lights in 1550 and 1060nm regions are used for mid-IR multiwavelength operation in a DFG laser source, it is better to choose a multiwavelength YDFL rather than a multiwavelength EDFL because the QPM BW for the pump light is larger than that for the signal light. This result is in agreement with our simulation results. Moreover, by replacing the used signal light EDFL with a DFB laser diode, mid-IR multiwavelength radiation is expected to be achieved in the same way, and then the mid-IR multiwavelength DFG laser source may find useful applications in multi-species detection as the DFB laser diode is easy to be modulated. It is also worthwhile to point out that high-efficiency robust mid-IR multiwavelength DFG source may be achieved when a waveguide PPLN is used instead of the bulk one in our experiment.

## 5. Conclusion

We have demonstrated a mid-IR multiwavelength DFG laser source with YDFL and EDFL as the fundamental lights by using the PPLN dispersion property to broaden the QPM wavelength acceptance bandwidth. Our simulation results show that, the QPM BWs for signal and pump lights are different. The QPM BW for the pump near 1060nm is much larger than that for signal near 1550nm. When the signal wavelength is fixed at 1560nm, by optimizing the crystal temperature the QPM BW for the pump is over 17nm, corresponding to the BW for the idler of about 180nm. Based on this principle, a multiwavelength YDFL and a single wavelength EDFL cascaded by an EDFA are respectively used as the pump and the signal lights, 14 mid-IR lasing lines with the spacing of 14nm are obtained simultaneously with our DFG laser source with a uniform grating period PPLN at a fixed temperature. Moreover, the mid-IR multiwavelength lasing lines may be tuned synchronously between 3.28 and 3.47 $\mu$ m by changing the signal wavelength. Such a mid-IR multiwavelength DFG laser source may find its applications in multiple species trace-gas detections in the future.

## Acknowledgments

This work is supported by the National Natural Science Foundation of China (Grant No. 60677050) and the National Basic Research Program of China (Grant No. 2007CB936603).